

Synthesis Design

2',4'-BNA/LNA with 9-(2-Aminoethoxy)-1,3-diaza-2-oxophenoxazine Efficiently Forms Duplexes and Has Enhanced Enzymatic Resistance**

Yuki Kishimoto,^[a, b] Osamu Nakagawa,^{*[a, b, d]} Akane Fujii,^[a, b] Kotaro Yoshioka,^[b, c]
Tetsuya Nagata,^[b, c] Takanori Yokota,^[b, c] Yoshiyuki Hari,^[d] and Satoshi Obika^{*[a, b]}

Abstract: Artificial nucleic acids are widely used in various technologies, such as nucleic acid therapeutics and DNA nanotechnologies requiring excellent duplex-forming abilities and enhanced nuclease resistance. 2'-O,4'-C-Methylene-bridged nucleic acid/locked nucleic acid (2',4'-BNA/LNA) with 1,3-diaza-2-oxophenoxazine (BNAP (B^H)) was previously reported. Herein, a novel B^H analogue, 2',4'-BNA/LNA with 9-(2-aminoethoxy)-1,3-diaza-2-oxophenoxazine (G-clamp), named BNAP-AEO (B^{AEO}), was designed. The B^{AEO} nucleoside was successfully synthesized and incorporated into oligodeoxynucleotides (ODNs). ODNs containing B^{AEO} possessed

up to 10^4 -, 152-, and 11-fold higher binding affinities for complementary (c) RNA than those of ODNs containing 2'-deoxycytidine (C), 2',4'-BNA/LNA with 5-methylcytosine (L), or 2'-deoxyribonucleoside with G-clamp (P^{AEO}), respectively. Moreover, duplexes formed by ODN bearing B^{AEO} with cDNA and cRNA were thermally stable, even under molecular crowding conditions induced by the addition of polyethylene glycol. Furthermore, ODN bearing B^{AEO} was more resistant to 3'-exonuclease than ODNs with phosphorothioate linkages.

Introduction

Artificial nucleic acids are widely used in DNA nanotechnologies^[1] and nucleic acid based therapies.^[2] The high duplex-forming ability of these artificial nucleic acids improves gene expression inhibition based oligonucleotide (ON) therapeutics.^[2] To maintain their activity within the cell, these ONs must be nuclease resistant.^[2] Briefly, the moieties modified for improving duplex stability and enzymatic resistance of nucleic acids include nucleobases, sugars, and the phosphate backbone. Among these, nucleobase modification can dramatically affect base recognition.^[3] The 1,3-diaza-2-oxophenoxazine (known as tCO or phenoxazine) artificial nucleobase is a tricyclic cytosine analogue that has been extensively studied for its ability to improve the thermal stability of a duplex (Fig-

ure 1 a).^[4] 9-(2-Aminoethoxy)-1,3-diaza-2-oxophenoxazine (G-clamp) has also been developed (Figure 1 b),^[5] to improve the π - π stacking interaction with adjacent bases and form additional hydrogen bonds with the 6-carbonyl group of guanine. Therefore, oligodeoxynucleotides (ODNs) that contain G-clamps could dramatically improve duplex-forming abilities. Based on the G-clamp design, several artificial nucleobases with expanded aromatic rings have been developed for improving π - π stacking interactions.^[6] Recently, we developed a novel phenoxazine analogue (1,3,9-triaza-2-oxophenoxazine (9-TAP)) with improved triplex-forming abilities^[7] and metal-mediated base pairs.^[8]

We recently developed a 2'-O,4'-C-methylene-bridged nucleic acid/locked nucleic acid (2',4'-BNA/LNA) with a tCO base (BNAP (B^H); Figure 2 c).^[9] 2',4'-BNA/LNA (Figure 2 a), which has a


[a] Dr. Y. Kishimoto, Dr. O. Nakagawa, A. Fujii, Prof. Dr. S. Obika
Graduate School of Pharmaceutical Sciences
Osaka University, 1-6 Yamadaoka Suita
Osaka 565-0871 (Japan)
E-mail: obika@phs.osaka-u.ac.jp


[b] Dr. Y. Kishimoto, Dr. O. Nakagawa, A. Fujii, Dr. K. Yoshioka, Dr. T. Nagata,
Prof. Dr. T. Yokota, Prof. Dr. S. Obika
Core Research for Evolutional Science and Technology (CREST)
(Japan) Sciences and Technology Agency (JST), 7 Gobancho
Chiyoda-ku, Tokyo 102-0076 (Japan)

[c] Dr. K. Yoshioka, Dr. T. Nagata, Prof. Dr. T. Yokota
Department of Neurology and Neurological Science
Graduate School of Medical and Dental Sciences
Tokyo Medical and Dental University
1-5-45 Yushima, Bunkyo-ku, Tokyo 113-8519 (Japan)

[d] Dr. O. Nakagawa, Prof. Dr. Y. Hari
Faculty of Pharmaceutical Sciences, Tokushima Bunri University
180 Nishihamahaji, Yamashiro-cho, Tokushima 770-8514 (Japan)
E-mail: osamu_nakagawa@ph.bunri-u.ac.jp

[**] 2',4'-BNA/LNA = 2'-O,4'-C-methylene-bridged nucleic acid/locked nucleic acid.

 Supporting information and the ORCID identification number(s) for the author(s) of this article can be found under:
<https://doi.org/10.1002/chem.202003982>

 © 2020 The Authors. Chemistry - A European Journal published by Wiley-VCH GmbH. This is an open access article under the terms of the Creative Commons Attribution Non-Commercial License, which permits use, distribution and reproduction in any medium, provided the original work is properly cited and is not used for commercial purposes.

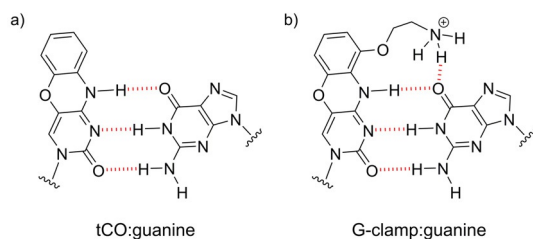


Figure 1. Base pairs of tCO:guanine (a) and G-clamp:guanine (b).

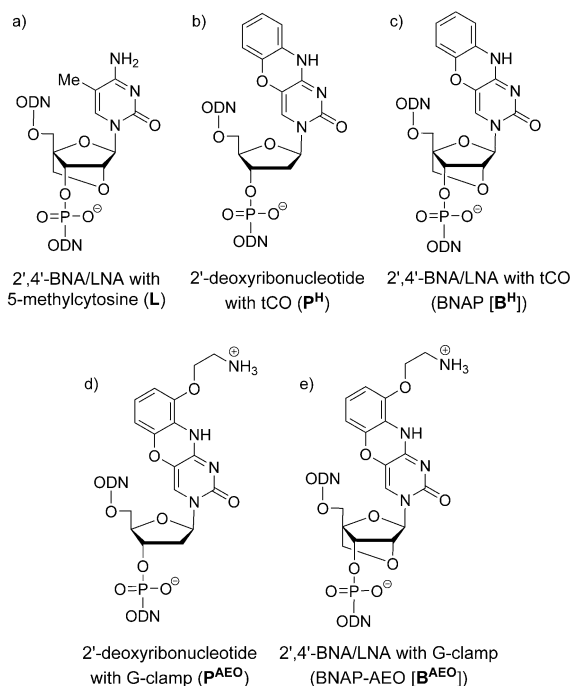


Figure 2. Structures of the artificial nucleic acids used in this study.

fixed N-type sugar conformation and improves duplex stability.^[10,11] The original design concept of 2',4'-BNA/LNA was to prevent entropy loss by preorganization into an N-type sugar conformation in A-form DNA duplexes. Another mechanism for improving duplex stability that improves the π - π stacking interaction with adjacent bases has been proposed.^[12] We expected that B^H , which combines 2',4'-BNA/LNA and a tCO base, would further improve duplex stability by increasing π - π stacking interactions. As expected, compound B^H showed high thermal stability relative to that of 2',4'-BNA/LNA with 5-methylcytosine (L) and 2'-deoxyribonucleoside with tCO (P^H).

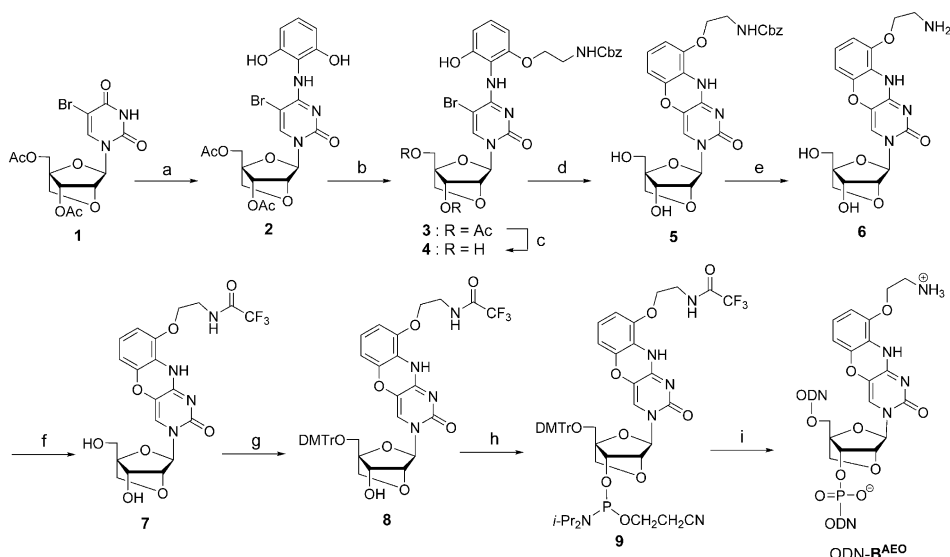
Herein, we developed a novel artificial nucleic acid that possessed excellent duplex-forming abilities and enhanced enzymatic resistance. We believe that such a nucleic acid will be a promising tool in DNA nanotechnologies and ON therapeutics. Based on this concept, we designed 2',4'-BNA/LNA with a G-clamp (BNAP-AEO (B^{AEO}); B^{AEO} means B^H with 2-aminoethoxy (AEO) at position 9; Figure 2e). Duplexes containing B^{AEO} were very stable.

Finally, we investigated the detailed properties of ODN- B^{AEO} , including its enzymatic resistance and fluorescence.

Results and Discussion

Synthesis of ODNs containing B^{AEO}

The B^{AEO} phosphoramidite (**9**), a precursor for incorporation into ODNs, was synthesized by using 2',4'-BNA/LNA and 5-bromouracil (**1**) as starting materials (Scheme 1 and Figure S1 in the Supporting Information). Compound **1** is an intermediate used for the synthesis of B^H ,^[9] the synthesis of **9** could be achieved according to the synthesis of B^H ^[9] and a 2'-deoxyribonucleoside with a G-clamp (P^{AEO}).^[5] First, compound **1** was chlorinated at position 4 by the Appel reaction with PPh_3 and CCl_4



Scheme 1. Synthesis of ODN containing B^{AEO} . Reagents and conditions: a) PPh_3 , CCl_4 , CH_2Cl_2 , reflux, 2 h, then 2-aminoresorcinol, 1,8-diazabicyclo[5.4.0]undec-7-ene (DBU), RT, 6 h (73%); b) benzyl-*N*-(2-hydroxyethyl)carbamate, diethyl azodicarboxylate (DEAD), PPh_3 , CH_2Cl_2 /THF, 0 °C → RT, 5 h (95%); c) 7 M NH_3 in MeOH, RT, 2 h; d) DBU, EtOH, reflux, 5 h (2 steps in 57%); e) $Pd(OH)_2/C$, cyclohexene, MeOH, reflux 5 h (93%); f) trifluoroacetic anhydride (TFAA), pyridine, 0 °C → RT, 2 h; g) 4,4'-dimethoxytrityl chloride (DMTrCl), silver trifluoromethanesulfonate (AgOTf), 2,6-lutidine, CH_2Cl_2 , 0 °C → RT, 2 h (2 steps, 47%); h) $iPr_2NP(=O)(Cl)OCH_2CH_2CN$, *N,N*-diisopropylethylamine (DIPEA), CH_2Cl_2 , RT, 2 h (77%); i) DNA synthesizer.

in CH_2Cl_2 , followed by the addition of 2-aminoresorcinol in the presence of DBU at reflux to obtain **2** (73% yield). Then, a benzyloxycarbonyl (Cbz)-protected aminoethanol unit was introduced to **2** by the Mitsunobu reaction by using DEAD, PPh_3 in $\text{CH}_2\text{Cl}_2/\text{THF}$ to obtain **3** (95%). The 3'- and 5'-diacetyl groups of **3** were removed by using a solution of ammonia in methanol to obtain **4**. The phenoxazine skeleton was constructed from **4** by using DBU in ethanol under reflux (57% in 2 steps). The Cbz group of 2-aminoethanol at position 9 of **5** was removed to obtain the B^{AEO} nucleoside (**6**). In ^1H NMR ($[\text{D}_6]\text{DMSO}$) spectroscopic analysis of **6**, two tautomers between the 10- and 1-positions in **6** were confirmed (ratio: 4/1 major ($\text{NH}(10)=\text{N}(1)$)/minor ($\text{N}(10)=\text{C}-\text{NH}(1)$)). Compound **6** was protected with a trifluoroacetyl group at the AEO moiety at the phenoxazine base to obtain **7**. Compound **7** was protected with a 4,4'-dimethoxytrityl group to acquire **8**, which was phosphorylated to obtain **9**.

Compound **9** was incorporated into an ODN by using an automated DNA/RNA synthesizer, with 5-[3,5-bis(trifluoromethyl)phenyl]-1*H*-tetrazole (Activator[®] 42) as an activator with a prolonged coupling time of 720 s (natural nucleoside: 30 s). Rapidly deprotected phosphoramidites (*N*-phenoxyacetyl (Pac)-2'-deoxyadenosine, *N*-*p*-isopropyl-Pac-2'-deoxyguanosine, and *N*-acetyl-2'-deoxycytidine) were used as the phosphoramidites of the natural 2'-deoxynucleosides of A, G, and C. The phosphoramidite of natural thymidine was used for T. Cleavage from the controlled pore glass (CPG) and deprotection of the ODNs containing B^{AEO} were carried out with a 50 mM solution of K_2CO_3 in methanol at room temperature for 4 h. We previously found that the deprotection of ODN-bearing B^{H} was effective in ammonium hydroxide/methylamine (AMA; v/v, 1:1) at 65 °C for 10 min.^[9] However, ODNs containing B^{AEO} decomposed under such conditions. Furthermore, the ODN-bearing B^{AEO} s with adjacent 5'- and 3'-purine bases (guanine and adenine) of B^{AEO}

tended to show increased decomposition under the AMA conditions. The ODNs containing B^{AEO} were purified by means of HPLC on a reverse-phase octadecylsilyl column (Figure S2 in the Supporting Information). The ODNs containing B^{AEO} were characterized by means of MALDI-TOF analysis (Table 1 and Figure S3 in the Supporting Information).

Table 1. Sequences and MALDI-TOF data for ODNs containing B^{AEO} .

Sequence	m/z [$M-H$] ⁻	
	Calcd	Found
5'-d(GCGTT B^{AEO} TTTGCT)-3'	3794.5	3793.8
5'-d(GCGTC B^{AEO} ATTGCT)-3'	3788.5	3788.4
5'-d(GCGTC B^{AEO} CTTGCT)-3'	3764.5	3763.6
5'-d(GCGTAB B^{AEO} ATTGCT)-3'	3812.6	3813.0
5'-d(GCGTGB B^{AEO} GTTGCT)-3'	3844.6	3744.2
5'-d(GCGTB B^{AEO} B^{AEO} TTGCT)-3'	3941.7	3942.6
5'-d(GCGTC B^{AEO} B^{AEO} TTGCT)-3'	3941.7	3940.4
5'-d(GCGTB B^{AEO} B^{AEO} B^{AEO} TTGCT)-3'	4118.8	4117.8
5'-d(TTTTTTTT B^{AEO})-3'	3141.1	3141.3

Thermal stabilities of duplexes containing B^{AEO} with multiple adjacent bases

The thermal stabilities of duplexes formed between ODNs containing B^{AEO} (12-mer) and complementary (c) DNA and RNA were investigated by using UV melting experiments (Table 2 and Figure S4 in the Supporting Information). The concept behind the design of B^{AEO} was to improve its duplex-forming ability by increasing guanine hydrogen bonding and π - π stacking interactions with adjacent nucleobases. Therefore, ODNs containing various 5'- and 3'-adjacent bases of B^{AEO} were evaluated. Melting temperatures (T_m) were determined at 260 nm in 2 mM sodium phosphate buffer (pH 7.2) containing

Table 2. The T_m values of duplexes formed by ODNs with cDNA and cRNA.^[a]

ODNs (5'-NNN-3')	T_m ($\Delta T_m = (T_m(\text{L}, \text{P}^{\text{AEO}}, \text{or } \text{B}^{\text{AEO}}) - T_m(\text{C}) / \text{modification})$ [°C]							
	X: C	L	Target DNA P^{AEO}	B^{AEO}	C	L	Target RNA P^{AEO}	B^{AEO}
TXT	40	44 (+4)	50 (+10)	53 (+13)	41	48 (+7)	52 (+11)	57 (+16)
CXA	44	48 (+4)	55 (+11)	53 (+9)	46	53 (+7)	59 (+13)	62 (+16)
CXC	45	51 (+6)	61 (+16)	64 (+19)	54	61 (+7)	67 (+13)	72 (+18)
AXA	41	45 (+4)	43 (+2)	42 (+1)	43 ^[b]	44 (+6)	56 (+13) ^[b]	61 (+18) ^[b]
GXG	46	48 (+2)	54 (+8)	51 (+5)	38	45 (+7)	45 (+7)	47 (+9)
XCX	45	55 (+5.0)	69 (+12.0)	75 (+15.0)	46	51 (+5)	48 (+2)	53 (+7)
CXX	45	53 (+4.0)	65 (+10.0)	63 (+9.0)	54	67 (+6.5)	74 (+10.0)	n.d.
XXX	45	58 (+4.3)	77 (+10.7)	70 (+8.3)	43 ^[b]	65 (+5.5)	62 (+9.5) ^[b]	73 (+15.0) ^[b]
					54	66 (+11.5) ^[b]	76 (+11.0)	80 (+13.0)
					43 ^[b]	71 (+5.7)	66 (+11.5) ^[b]	68 (+12.5) ^[b]
					54		n.d.	n.d.
					43 ^[b]		74 (+10.3) ^[b]	76 (+11.0) ^[b]

[a] UV melting profiles were measured in 2 mM sodium phosphate buffer (pH 7.2) containing 20 mM NaCl at a scan rate of 0.5 °C min⁻¹ at 260 nm. The concentration of ON was 2 μM for each strand. The error in T_m was ± 0.5 °C. [b] Measured under non-NaCl conditions. C: 2'-deoxycytidine, L: 2',4'-BNA/LNA with 5-methylcytosine, P^{AEO} : 2'-deoxyribonucleoside with G-clamp, B^{AEO} : BNAP-AEO. Sequence: 5'-d(GCGTNNNTTGCT)-3'/3'-CGCAQQQAACGA-5' (X (in N): C, L, P^{AEO} or B^{AEO} , Q: corresponding matching base); n.d.: not determined.

20 mM sodium chloride. The concentration of each ODN was 2 μM . ODNs containing **L** or **P^{AEO}** were also investigated as controls. Thereafter, ODN-**X** and duplex-**X** indicate ODN and a duplex containing **X**, respectively, in which **X** represents **C**, **P^{AEO}**, or **B^{AEO}**. To depict the 5'- and 3'-adjacent bases of **X** in ODN-**X**, the notation ODN(NXN) is used (**N** is one of the four natural nucleobases, adenine (A), guanine (G), cytosine (C), or thymine (T) as 5'- and 3'-adjacent bases of **X**). For example, ODN(TB^{AEO}T) means ODNs containing 5'- and 3'-adjacent TT bases of **B^{AEO}**. ODN(NXN)/cDNA and ODN(NXN)/cRNA indicate the duplex formed with cDNA and cRNA, respectively. ΔT_m is the difference between the T_m value of **X** and the T_m value of **C**, unless otherwise noted.

First, the thermal stabilities of ODN(TXT)/cDNA were measured. The T_m value of ODN(TB^{AEO}T)/cDNA was 53 °C, which was 13 °C higher than that of ODN(TCT)/cDNA. Furthermore, the T_m value of ODN(TB^{AEO}T)/cDNA was 9 and 3 °C higher than those of ODN(TLT) and ODN(TP^{AEO}T), respectively. For ODN(TXT)/cDNA, the T_m values decreased in the order of **B^{AEO}** > **P^{AEO}** > **L** > **C**. For adjacent CC bases, the T_m value of ODN(CB^{AEO}C)/cDNA was 64 °C. The T_m value of ODN(CB^{AEO}C)/cDNA was 19 °C, which was much higher than that of ODN(CCC)/cDNA. The ΔT_m value of ODN(CB^{AEO}C)/cDNA was 6 °C higher than that of ODN(TB^{AEO}T)/cDNA. The thermal stability of ODN(CXC)/cDNA decreased in the order of **B^{AEO}** > **P^{AEO}** > **L** > **C**. The thermal stability of ODN-B^{AEO}/cDNA was effectively improved if the 5'- and 3'-adjacent base of **B^{AEO}** was CC rather than TT ($\Delta T_m = +19$ °C (CB^{AEO}C), $+13$ °C (TB^{AEO}T)). In contrast, the ΔT_m value of ODN(CB^{AEO}A)/cDNA decreased by 10 °C compared with that of ODN(CB^{AEO}C)/cDNA and was 2 °C lower than that of ODN(CP^{AEO}A)/cDNA. For adjacent AA bases of **B^{AEO}**, ODN(AB^{AEO}A)/cDNA did not improve the T_m , which was lower than those of ODN(ALA)/cDNA and ODN(AP^{AEO}A)/cDNA (**L** > **P^{AEO}** > **B^{AEO}** > **C**). For adjacent GG **B^{AEO}** bases, the T_m value of ODN(GB^{AEO}G)/cDNA was 51 °C, which was 5 and 3 °C higher than those of ODN(GCG)/cDNA and ODN(GLG)/cDNA, respectively. However, the T_m value of ODN(GB^{AEO}G)/cDNA was not improved over that of ODN(GP^{AEO}G) ($\Delta T_m(\text{B}^{\text{AEO}}-\text{P}^{\text{AEO}}) = -3$ °C). Thus, derivative **B^{AEO}** led to an excellent performance with pyrimidine (especially C rather than T) bases at both 5'- and 3'-adjacent bases. In our previous study on **B^H**, the thermal stability of ODN/DNA duplexes containing **P^H** and **B^H** also improved with adjacent pyrimidines (C and T) rather than purines (A and G; Table S2 in the Supporting Information).^[9]

We investigated ODNs containing two or three continuous modifications (**X**; ODN(CXX), ODN(XXX)), which were expected to improve π - π stacking interactions between **B^{AEO}**s. With such modifications, ODN(CB^{AEO}B^{AEO})/cDNA and ODN(B^{AEO}B^{AEO}B^{AEO})/cDNA increased the T_m values, compared with those of ODN(CLL)/cDNA and ODN(LLL)/cDNA, respectively. However, ODN(CB^{AEO}B^{AEO})/cDNA and ODN(B^{AEO}B^{AEO}B^{AEO})/cDNA had slightly lower T_m values than those of ODN(CP^{AEO}P^{AEO})/cDNA and ODN(P^{AEO}P^{AEO}P^{AEO})/cDNA. The T_m value of ODN-B^{AEO}/cDNA was not improved by continuous modifications in comparison with single modifications, such as ODN(TB^{AEO}T)/cDNA and ODN(CB^{AEO}C)/cDNA. In contrast, for ODN(B^{AEO}CB^{AEO})/cDNA containing two one-interval modification of **B^{AEO}** maintained the

high T_m value of the single modifications of ODN(TB^{AEO}T)/cDNA and ODN(CB^{AEO}C)/cDNA.

The thermal stabilities of ODN-B^{AEO}s and cRNA were also measured. Overall, ODN-B^{AEO}/cRNA had a higher thermal stability than that of ODN-B^{AEO}/cDNA ($\Delta T_m = +7$ (+18 °C for cRNA)). ODN-B^{AEO}/cRNA showed excellent thermal stability compared with ODN-C/cRNA, ODN-L/cRNA, and ODN-P^{AEO}/cRNA derivatives, even with adjacent purine bases of **B^{AEO}**. ODN-B^{AEO}/cRNA with 5'-adjacent pyrimidines possessed an unusually high thermal stability ($\Delta T_m = +16$ -+18 °C). In the case of two one-interval modifications (XCX) and two or three continuous modifications (CXX or XXX), ODN-B^{AEO}/cRNA maintained the high duplex-forming ability that was observed with one modification ($\Delta T_m/\text{modification} = +11$ -+15 °C). For the extremely high thermal stabilities observed for multiple **B^{AEO}** modifications, T_m was redetermined under non-NaCl conditions. In the case of continuous modifications, ODN-B^{AEO}/cRNA demonstrated an advantage over ODN-B^{AEO}/cDNA. Moreover, even in the case of adjacent purines, ODN-B^{AEO}/cRNA performed better than ODN-B^{AEO}/cDNA.

According to the study reported by Ortega et al., we also analyzed ODN-B^{AEO}s using their sequence and buffer (Table S7 in the Supporting Information).^[5b] Under these conditions, the ΔT_m values of ODN(CB^{AEO}C)/cDNA and ODN(CP^{AEO}C)/cDNA were +22 and +17 °C, respectively. Furthermore, the ΔT_m values of ODN(CB^{AEO}C)/cRNA and ODN(CP^{AEO}C)/cRNA were +20 and +15 °C, respectively. The high thermal stability of duplex **B^{AEO}** was maintained under these conditions.

Thus, duplex **B^{AEO}** showed excellent thermal stability in comparison with those of duplexes **C**, **L**, and **P^{AEO}**. We previously reported the thermal stabilities of duplexes **P^H** and **B^H** with the same sequence and under the same conditions (Table S2 in the Supporting Information).^[9] With 5'-pyrimidine adjacent bases of **B^H** in the duplex, duplex **B^H** and duplex **B^{AEO}** showed excellent thermal stability. In summary, the order of thermal stabilities of duplex with 5'-pyrimidine adjacent bases was **B^{AEO}** > **P^{AEO}** > **B^H** > **L** > **C**.

Mismatch discrimination ability of **B^{AEO}** in duplexes

We investigated the mismatch discrimination ability of **B^{AEO}** in ODN/DNA and ODN/RNA (Table 3 and Figure S6 in the Supporting Information). ODN(CXC) with 5',3'-adjacent CC bases were used because the sequence showed high thermal stabilities in the above experiment.

The **B^{AEO}** derivative showed excellent base discrimination ($\Delta T_m(\text{B}^{\text{AEO}}) = -26$ (A-G), -29 (T-G), -36 °C (C-G)) in ODN/DNA. The mismatched T_m values of ODN-B^{AEO}/DNA were +6 (A), +6 (T), and +4 °C (C) higher than those of ODN-C/DNA. If comparing **B^{AEO}** and **L**, the matched T_m value of ODN-B^{AEO}/DNA was high (+13 °C); in contrast, the mismatched T_m values of ODN-B^{AEO}/DNA were similar to those of ODN-L/DNA ($\Delta T_m = +1$ (A), +2 (T), +1 °C (C)). The mismatched T_m value of ODN-B^{AEO}/DNA was nearly identical to that of ODN-P^{AEO}/DNA. Thus, ODN-B^{AEO}/DNA demonstrated high thermal stability in cases of matched G, but dramatically reduced thermal stability in the presence of mismatched bases.

Table 3. A comparison of matched versus mismatched hybridization.^[a]

X	5'-d(GCGTCXCTTGCT)-3' 3'-d(CGCAGYGAACGA)-5'				
	Y:	G	A	T	C
C		45	32 (-13)	29 (-16)	24 (-21)
L		51	37 (-14)	33 (-18)	27 (-24)
P ^{AEO}		61	38 (-23)	34 (-27)	24 (-37)
B ^{AEO}		64	38 (-26)	35 (-29)	28 (-36)
X	5'-d(GCGTCXCTTGCT)-3' 3'-r(CGCAGYGAACGA)-5'				
	Y:	G	A	U	C
C		54	39 (-15)	31 (-23)	32 (-22)
L		61	45 (-16)	40 (-21)	38 (-23)
P ^{AEO}		67	44 (-23)	41 (-26)	38 (-29)
B ^{AEO}		72	47 (-25)	45 (-27)	42 (-30)

[a] Values in parentheses are the difference between T_m if the ODN is bound to the guanine-containing target and T_m if the ODN is bound to a mismatched base. The buffer conditions were the same as those given in Table 2.

For ODN/RNA, the B^{AEO} derivative also showed excellent base discrimination ($\Delta T_m(\text{B}^{\text{AEO}}) = -25$ (A-G), -27 (U-G), -30 °C (C-G)). However, unlike in ODN-B^{AEO}/DNA, the T_m values of ODN-B^{AEO}/RNA compared with those of ODN-C/RNA increased with mismatched bases ($\Delta T_m = +8$ (A), $+14$ (U), $+10$ °C (C) in RNA). In contrast, the base discrimination of B^{AEO} slightly decreased compared with that of L ($\Delta T_m(\text{B}^{\text{AEO}}\text{-L})$: $+2$ (A), $+5$ (U), $+4$ °C (C) in RNA).

We previously reported the base discrimination of B^H in a duplex (Table S3 in the Supporting Information).^[9] The base discrimination ability of B^H was lower than that of B^{AEO}. With mismatched A and T (or U), the T_m value of duplex-B^H was higher than that of duplex B^{AEO} ($\Delta T_m(\text{B}^{\text{AEO}}\text{-B}^{\text{H}}) = -1$ (A), -4 (T), $+2$ °C (C) with DNA), suggesting that the tCO base without an AEO unit had low discrimination abilities. The AEO group may contribute significantly to the high base-discrimination ability of tCO analogues. Thus, the B^{AEO} derivative possesses excellent base-discrimination abilities in both ODN/DNA and ODN/RNA.

Circular dichroism (CD) analysis of duplexes containing B^{AEO}

The structure of duplex B^{AEO} was investigated by using CD (Figure 3). Measurements were performed by using the same buffer conditions as those used for UV melting experiments.

The formation of the ODN(CB^{AEO}C)/cDNA duplex did not induce large conformational changes in comparison with those of ODN(CCC)/cDNA. ODN(CB^{AEO}C)/cDNA maintained a typical B-form DNA/DNA structure. Furthermore, ODN(CB^{AEO}C)/cRNA, similar to ODN(CCC)/cRNA, maintained an A-form duplex. Thus, the duplexes formed between adjacent CC bases of B^{AEO} did not undergo large conformational changes.

We also investigated the duplex structures of ODN(AB^{AEO}A) using cDNA and cRNA (Figure S7 in the Supporting Information). The structure of ODN(AB^{AEO}A)/cDNA was slightly different from the typical B-form structure observed with ODN(ACA)/cDNA. Furthermore, ODN(AB^{AEO}A)/cRNA possessed small con-

formational changes that were not present in the A-form of ODN(ACA)/cRNA.

Thus, the observation that duplexes of B^{AEO} with adjacent CC result in no conformational changes reveal that the presence of B^{AEO} in duplexes may contribute to the maintenance of B- and A-form structures with high thermal stability. On the contrary, duplexes of B^{AEO} with adjacent AA bases showed a small conformational change; therefore, the thermal stabilities of duplex B^{AEO} with adjacent AA might be decreased compared with those of duplex B^{AEO} with adjacent CC.

Molecular dynamics (MD) analyses of duplexes containing B^{AEO}

We investigated the structure of duplex B^{AEO} by MD calculations using 12-mers of ODN(CB^{AEO}C)/cDNA and ODN(CB^{AEO}C)/cRNA (Figure 4 and Figure S8 in the Supporting Information).

The structure of ODN(CB^{AEO}C)/cDNA was maintained in typical B-form duplexes without distortion around B^{AEO} (Figure 4a). The G-clamp base moiety in B^{AEO} effectively overlapped with the 5'-adjacent cytosine base (Figure 4b). In contrast, the G-clamp base in B^{AEO} did not sufficiently overlap with the 3'-adjacent cytosine. The A-form duplex was maintained with ODN(CB^{AEO}C)/cRNA, without disturbing the structure around B^{AEO} (Figure S8 in the Supporting Information). The overlap between the B^{AEO} base and the 5'-adjacent C base tended to be larger in DNA/DNA than that in DNA/RNA. In other words, the overlap between bases was more apparent in B-form than in A-form duplexes.^[9] Therefore, the adjacent base independence of B^{AEO} might be smaller in the B-form than in A-form duplexes. These simulation MD results were in good agreement with the experimental CD measurements.

Thermodynamic parameters of duplexes containing B^{AEO}

To verify the molecular mechanism underlying the improved stability of duplex B^{AEO}, thermodynamics parameters were ob-

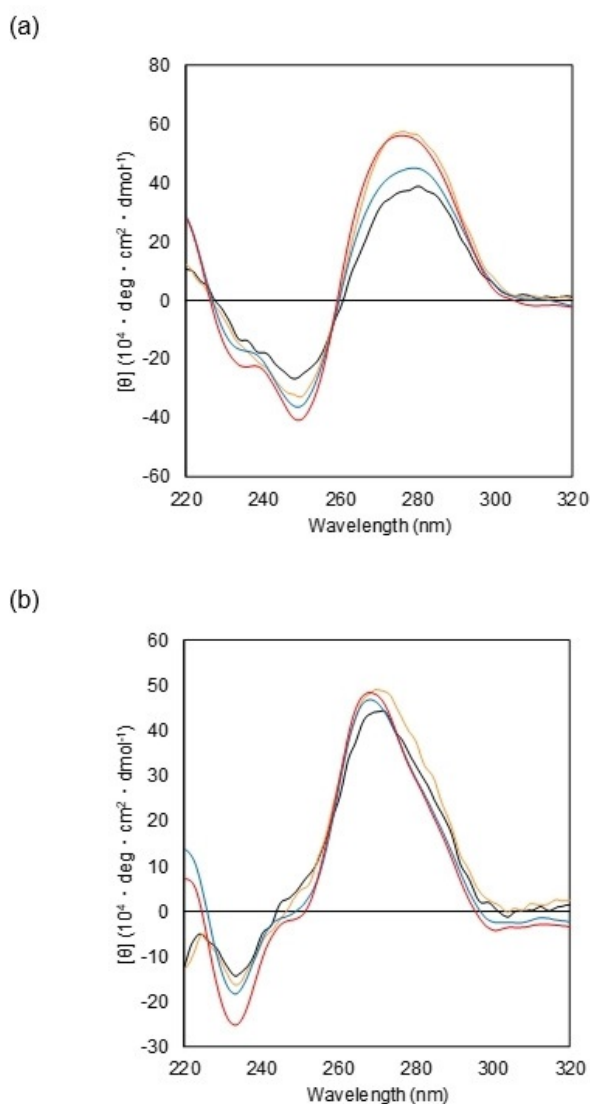


Figure 3. CD spectra of ODN(CXC)/cDNA (a) and ODN(CXC)/cRNA (b) duplexes. Conditions: 2 mM sodium phosphate buffer (pH 7.2), 20 mM NaCl, 2 μ M each strand. C: black, L: orange, P^{AEO}: blue, B^{AEO}: red. Sequence: 5'-d(GCGTCXCTTGCT)-3'/3'-CGCAGGGAACGA-5' (X: C, L, P^{AEO}, or B^{AEO}).

tained from van't Hoff plots based on the T_m results obtained at multiple concentrations (Table 4 and Table S4 and Figure S9 in the Supporting Information).

For adjacent CC bases, ODN-B^{AEO}/cDNA showed a favorable entropy change ($\Delta\Delta H = +14.1$ kcal mol⁻¹, $\Delta\Delta S = +57$ cal mol⁻¹ K⁻¹); $\Delta\Delta H$, $\Delta\Delta S$, or $\Delta\Delta G$ indicate differences from the cor-

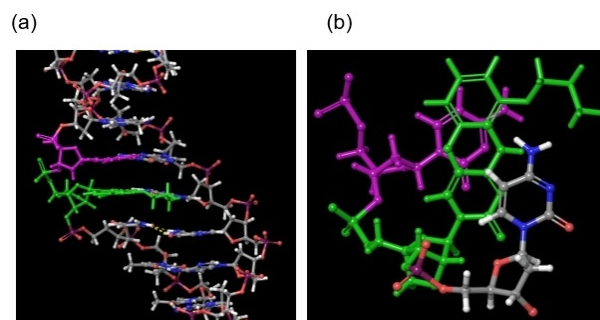


Figure 4. Snapshot of MD analysis of the ODN(CB^{AEO})/cDNA duplex. Left: side view; right: expanded top view of part of CB^{AEO}. MD calculations were performed with MacroModel software (Schrödinger, LLC) and the OPLS3 force field (in water at 300 K for 20 ns). Purple: 5'-adjacent cytidine to B^{AEO}, green: B^{AEO}. Sequence: 5'-d(GCGTCB^{AEO}CTTGCT)-3'/3'-d(CGCAGGGAACGA)-5'.

responding ΔH , ΔS , or ΔG values obtained for ODN-C/cDNA or cRNA. ODN-P^{AEO}/cDNA and ODN-L/cDNA also showed favorable changes in entropy. Therefore, the modifications of L, P^{AEO}, and B^{AEO} into ODN/DNA might use the same mechanisms for stabilizing duplexes. Thus, both the G-clamp and 2',4'-BNA/LNA moiety in B^{AEO} were associated with duplex stability.

ODN-B^{AEO}/cRNA had a favorable change in enthalpy that was different from that of ODN-B^{AEO}/cDNA ($\Delta\Delta H = -5.6$ kcal mol⁻¹, $\Delta\Delta S = +1$ cal mol⁻¹ K⁻¹); ODN-P^{AEO}/cRNA also showed this pattern ($\Delta\Delta H = -4.0$ kcal mol⁻¹, $\Delta\Delta S = +1$ cal mol⁻¹ K⁻¹), whereas ODN-L/cRNA had a substantial favorable change in enthalpy and an unfavorable change in entropy ($\Delta\Delta H = -7.2$ kcal mol⁻¹, $\Delta\Delta S = -15$ cal mol⁻¹ K⁻¹). The B^{AEO} and P^{AEO} derivatives had similar patterns in ODN/RNA; therefore, the G-clamp was expected to be a predominant influence, rather than that of 2',4'-BNA/LNA in B^{AEO}.

By comparing L and P^H in previous thermodynamic analyses of B^H, we determined that the tCO moiety of B^H primarily functioned in DNA/DNA, whereas 2',4'-BNA/LNA primarily functioned in DNA/RNA (Table S4 in the Supporting Information).^[9] Therefore, the mechanisms by which B^H and B^{AEO} confer duplex stability are different.

Next, the free energy changes of B^{AEO} duplexes were calculated ($\Delta\Delta G(X-C, cDNA) = -3.8$ (B^{AEO}), -3.2 (P^{AEO}), -1.1 kcal mol⁻¹ (L); $\Delta\Delta G(X-C, cRNA) = -5.7$ (B^{AEO}), -4.2 (P^{AEO}), -2.6 kcal mol⁻¹ (L)). The B^{AEO} derivative in ODN/RNA was stable, relative to that in ODN/DNA.

The binding constants (K_s) of ODN-B^{AEO} with cDNA and cRNA were calculated by using the above thermodynamic parame-

X =	Target DNA				Target RNA			
	ΔH [kcal mol ⁻¹]	ΔS [cal mol ⁻¹ K ⁻¹]	$\Delta G_{(37^\circ\text{C})}$ [kcal mol ⁻¹]	K_s [M ⁻¹]	ΔH [kcal mol ⁻¹]	ΔS [cal mol ⁻¹ K ⁻¹]	$\Delta G_{(37^\circ\text{C})}$ [kcal mol ⁻¹]	K_s [M ⁻¹]
C	-93.3	-265	-11.0	5.65×10^7	-97.4	-271	-13.4	2.77×10^9
L	-78.2	-213	-12.1	3.37×10^8	-104.6	-286	-16.0	1.89×10^{11}
P ^{AEO}	-79.8	-211	-14.2	1.02×10^{10}	-101.4	-270	-17.6	2.53×10^{12}
B ^{AEO}	-79.2	-208	-14.8	2.69×10^{10}	-103.0	-270	-19.1	2.88×10^{13}

[a] Sequence: 5'-d(GCGTCXCTTGCT)-3'/3'-CGCAGGGAACGA-5' (X: C, L, P^{AEO}, or B^{AEO}).

ters. The K_s value of ODN-**B**^{AEO} with cDNA was $2.69 \times 10^{10} \text{ M}^{-1}$. This value was about 480 times higher than that of ODN-**C**. In contrast, the K_s value of ODN-**L** was only sixfold higher than that of ODN-**C**. As a result, the K_s value of ODN-**B**^{AEO} was 80-fold higher than that of ODN-**L**. Furthermore, the K_s value of ODN-**B**^{AEO} was shown to be only 2.6-fold higher than that of ODN-**P**^{AEO}.

With respect to cRNA, ODN-**B**^{AEO} exhibited an extremely high binding affinity ($K_s = 2.88 \times 10^{13} \text{ M}^{-1}$), approximately 10^4 -fold higher than that of ODN-**C**. The binding affinities of ODN-**L** and ODN-**P**^{AEO} were 68 and 913 times higher than that of ODN-**C**. This suggests that ODN-**B**^{AEO} had K_s values 152- and 11-fold higher than those of ODN-**L** and ODN-**P**^{AEO}, respectively.

We also calculated the K_s value of ODN-**B**^H with cDNA and cRNA (Table S4 in the Supporting Information). ODN-**B**^{AEO}s had significantly higher binding affinities than that of ODN-**B**^H. Thus, in terms of K_s , the stability conferred by these modifications decreased in the order of **B**^{AEO} > **P**^{AEO} > **B**^H > **P**^H > **L** > **C**. These results clearly show that the introduction of **B**^{AEO} into the duplex dramatically improved the high duplex-forming ability in ODN/DNA and ODN/RNA.

Thermal stabilities of duplexes containing **B**^{AEO} under molecular crowding conditions

To evaluate the thermal stabilities of duplexes of **B**^{AEO} under molecular crowding conditions,^[13] UV melting experiments were performed in a buffer with or without 40 wt% polyethylene glycol (PEG)-200 (Table 5). In this section, ΔT_m represents the difference between T_m of ODN-**X**/cDNA (or cRNA) and that of ODN-**C**/cDNA (or cRNA) under the same buffer conditions. In other words, this ΔT_m refers to the thermal stabilization of each modification, **L**, **P**^{AEO} or **B**^{AEO}, compared with **C**. First, it was found that the thermal stabilization of ODN-**L**/cDNA did not change in the absence or presence of PEG ($\Delta T_m = +6$ and $+7^\circ\text{C}$, respectively); the same was observed for ODN-**L**/cRNA ($\Delta T_m = +9$ and $+9^\circ\text{C}$). ODN-**P**^{AEO} showed high thermal stabilization under the PEG(−) condition ($\Delta T_m = +15$ (cDNA) and $+14^\circ\text{C}$ (cRNA)), which was greater than that of ODN-**L**. Notably, the ΔT_m values under the PEG(+) condition ($+11$ (cDNA)

and $+9^\circ\text{C}$ (cRNA)) were 4 and 5°C lower than the ΔT_m values under the PEG(−) condition. On the other hand, ODN-**B**^{AEO} showed even better thermal stabilization: the ΔT_m values under the PEG(−) condition were $+18$ (cDNA) and $+19^\circ\text{C}$ (cRNA); under the PEG(+) condition, the ΔT_m values were $+16$ (cDNA) and $+17^\circ\text{C}$ (cRNA). Thus, the excellent thermal stabilization of ODN-**B**^{AEO} was maintained, even under molecular crowding conditions.

These results suggest that artificial nucleobases, which have increased π - π stacking interactions, have disadvantages when it comes to changes in the surrounding conditions. The stabilization effects of duplexes of **P**^{AEO} and **B**^{AEO} were different under buffer conditions used by us and Ortega et al.^[5b] (Table S7 in the Supporting Information). In duplexes of **B**^{AEO}, the π - π stacking function of G-clamp bases could be successfully overcome by the addition of 2',4'-BNA/LNA. As such, we expect ODN-**B**^{AEO} to be useful in cellular environments, such as for ON-based therapies.

Thermal stabilities of **B**^{AEO}-modified duplexes with mismatched adjacent base pairs

We measured how the mismatched 5'- and 3'-adjacent base pairs of **B**^{AEO}:G in ODN/DNA affected thermal stability (Table 6 and Table S5 in the Supporting Information). The **B**^{AEO} derivative was designed to enhance duplex-forming ability through increased π - π stacking interactions with adjacent bases in duplexes. Therefore, we hypothesized that adjacent, mismatched base pairs of **B**^{AEO}:G in the duplex would decrease π - π stacking interactions and, therefore, reduce duplex stability. In the case of 5'-mismatched base pairs (C:A, C:T, and C:C), the T_m value effectively decreased ($\Delta T_m(\text{mismatch-match}) = -24$ (C:A), -35 (C:T), -39°C (C:C)). Mismatched 5'-adjacent base pairs of **B**^{AEO}:G largely decreased T_m compared with those of C:G. For mismatched 3'-adjacent base pairs of **X**:G, ODN-**B**^{AEO}/DNA decreased T_m ($\Delta T_m(\text{mismatch-match}) = -22$ (C:A), -25 (C:T), -25°C (C:C), for **B**^{AEO}). Thermal stabilities of ODN-**B**^{AEO}/DNA effectively decreased with 5'-mismatch base pairs rather than 3'-mismatch base pairs ($\Delta T_m = -24$ to -39°C (5'-mismatch), -22 to -25°C (3'-mismatch)). The G-clamp base in **B**^{AEO} can overlap more effectively with 5'-adjacent matched base pairs than that of 3'-adjacent matched base pairs (Figure 4). It was expected that the G-clamp base in **B**^{AEO} effectively inhibited overlap for π - π stacking interactions with 5'-unstable mismatched base pairs.

Thus, the π - π stacking ability of **B**^{AEO} in the duplex is destabilized, even if adjacent base pairs are mismatched. This property is likely to be useful for technologies that require high sequence discrimination.

Fluorescence measurements of ODNs containing **B**^{AEO}

The tCO and G-clamp bases are known to fluoresce at 450 nm with 360 nm excitation.^[14] We investigated the fluorescence properties of ODN-**B**^{AEO} with/without target DNA and RNA (Figure 5). The fluorescence intensity change of **B**^{AEO} by base discrimination was also measured. Single-stranded ODN-**B**^{AEO}

X	T_m ($\Delta T_m = T_m(\text{L, P}^{\text{AEO}}, \text{ or B}^{\text{AEO}}) - T_m(\text{C})$) [$^\circ\text{C}$]			
	Target DNA		Target RNA	
	PEG (−)	PEG (+)	PEG (−)	PEG (+)
C	55	43	61	49
L	61 (+6)	50 (+7)	70 (+9)	58 (+9)
P ^{AEO}	70 (+15)	54 (+11)	75 (+14)	58 (+9)
B ^{AEO}	73 (+18)	59 (+16)	80 (+19)	66 (+17)

[a] UV melting profiles were measured in 10 mM tris(hydroxymethyl)aminomethane (Tris)/HCl buffer (pH 7.2) containing 40% PEG-200 and 100 mM KCl at a scan rate of $0.5^\circ\text{C min}^{-1}$ at 260 nm. The concentration of ON was $2 \mu\text{M}$ for each strand. The error in T_m values was $\pm 0.5^\circ\text{C}$. Sequence: 5'-d(GCGTCXCTTGCT)-3'/3'-CGCAGGGAACGA-5' (X: **C**, **L**, **P**^{AEO}, or **B**^{AEO}).

Table 6. T_m values of B^{AEO} -modified duplexes with 5'- and 3'-adjacent mismatch base pairs.^[a]

● X ● : Mismatched base pair ● : Matched base pair

Sequence 5'-CXC-3'/3'-GYG-5'

		X: C	T_m ($\Delta T_m = T_m(\text{mismatch}) - T_m(\text{match})$) [°C]		B^{AEO}
			L	P^{AEO}	
match	CXC	45	51	61	64
	GGG				
	CXC	29 (-16)	31 (-20)	39 (-22)	40 (-24)
	AGG				
5'-mismatch	CXC	21 (-24)	25 (-26)	27 (-34)	29 (-35)
	TGG				
	CXC	20 (-25)	17 (-34)	24 (-37)	25 (-39)
	CGG				
	CXC	31 (-14)	35 (-16)	39 (-22)	42 (-22)
3'-mismatch	GGA				
	CXC	32 (-13)	34 (-17)	37 (-24)	39 (-25)
	GGT				
	CXC	29 (-16)	34 (-17)	37 (-24)	39 (-25)
	GGC				

[a] The buffer conditions were the same as those given in Table 2.

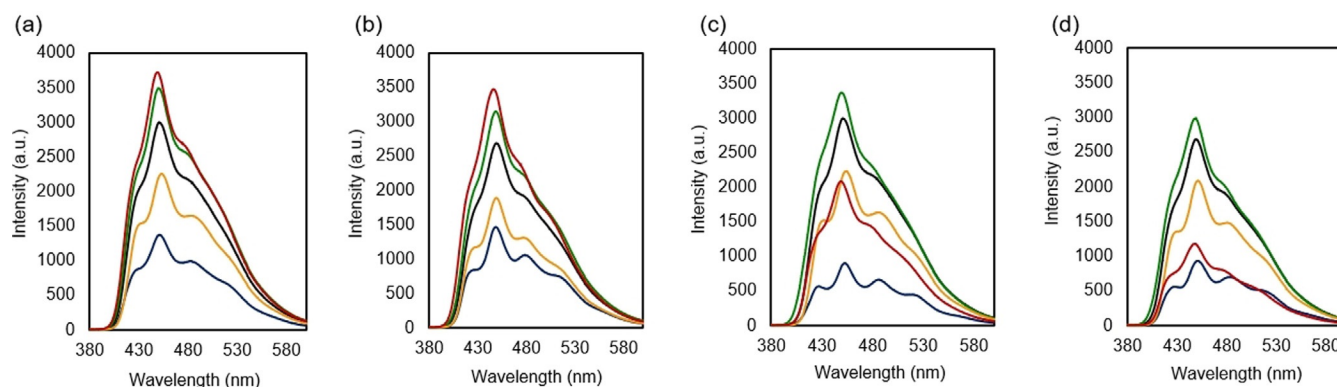


Figure 5. Fluorescence spectra of ODN- B^{AEO} /DNA (a), ODN- P^{AEO} /DNA (b), ODN- B^{AEO} /RNA (c), and ODN- P^{AEO} /RNA (d) duplexes. Conditions: 2 mM sodium phosphate buffer (pH 7.2), 20 mM NaCl, 2 μ M each strand. Sequence: 5'-d(GCGTCXCTTGCT)-3'/3'-CGCAGYGAACGA-5' (X: P^{AEO} or B^{AEO}). Black: single-stranded ODN. X:Y = X:A (dark blue), X:G (orange), X:C (green), X:T (or X:U) (red).

possessed a similar fluorescence pattern to that of ODN- P^{AEO} (maximum emission: 450 nm, excitation: 360 nm), although the fluorescence intensity of ODN- B^{AEO} was slightly smaller than that of ODN- P^{AEO} . The fluorescent base discrimination of B^{AEO} in duplexes was measured with matched G and mismatched A, T, and C. The fluorescence intensities of B^{AEO} were in the following descending order: duplex(B^{AEO} :T) > duplex(B^{AEO} :C) > single-stranded ODN- B^{AEO} > duplex(B^{AEO} :G) > duplex(B^{AEO} :A). This result was similar to that obtained for P^{AEO} , except that the intensity of the B^{AEO} :G duplex was slightly higher than that of P^{AEO} :G.

The fluorescence properties of B^{AEO} in ODN/RNA were also evaluated. The fluorescence intensity pattern of ODN- B^{AEO} /RNA was different from that of ODN- B^{AEO} /DNA and followed the order B^{AEO} :C duplex > single-strand ODN- B^{AEO} > B^{AEO} :G duplex > B^{AEO} :U duplex > B^{AEO} :A duplex. In contrast, the intensity differences between the B^{AEO} :U and P^{AEO} :U duplexes were slightly different in ODN/RNA.

The quenching mechanism of nucleobase fluorescence is generally known to be based on photoinduced electron transfer (PeT)^[16] and fluorescence resonance energy transfer (FRET).^[14] The main mechanism of fluorescence quenching of G-clamp is expected to be PeT.^[16] The PeT quenching ability is based on the electrochemical oxidation potentials of the nucleobase (in order of G > A > C \approx T).^[17] In this study, duplexes with A and G in the opposite bases of P^{AEO} and B^{AEO} tended to show effective fluorescence quenching. Despite P^{AEO} and B^{AEO} having the same fluorophore as that of the G-clamp base, each duplex containing P^{AEO} and B^{AEO} showed different fluorescence intensities and patterns. It was reported that 2',4'-BNA/LNA could improve π - π stacking interactions with adjacent bases in the duplex.^[12] This difference in fluorescence between B^{AEO} and P^{AEO} is expected to be caused by changes in π - π stacking interactions and the surrounding structure induced by the 2',4'-BNA/LNA sugar. Furthermore, the fluorescence patterns of B^{AEO} and P^{AEO} were different, even between ODN/DNA

(B-form) and ODN/RNA (A-form). This might be induced by the difference in π - π stacking interactions of 5'- and 3'-adjacent bases of \mathbf{B}^{AEO} and \mathbf{P}^{AEO} in the B-form and A-form duplexes.

Enzymatic resistance of ODNs containing \mathbf{B}^{AEO}

We investigated the exonuclease resistance of \mathbf{B}^{AEO} in ODN. A 3'-exonuclease (*Crotalus adamanteus* venom phosphodiesterase) was used against a 10-mer ODN (5'-TTTTTTTTT \mathbf{B}^{AEO} -3'; Figure 6). ODNs containing **L**, \mathbf{P}^{AEO} , and two PS linkages (S_p and R_p isomers) were used as controls. About 80% of the full-length ODN- \mathbf{B}^{AEO} remained intact under these harsh conditions, in contrast to natural ODN-C, which was completely degraded within 10 min. Under these conditions, the full-length ODN- \mathbf{P}^{AEO} , ODN-**L**, and ODN- \mathbf{P}^{AEO} were maintained at 5, 20, and 52%, respectively. We confirmed that ODN- \mathbf{P}^{AEO} was known to have resistance against 3'-exonuclease.^[15] The resistance of ODN- \mathbf{B}^{AEO} was similar to that of ODN- \mathbf{P}^{AEO} . This result suggests that the high enzymatic resistance of \mathbf{B}^{AEO} was conferred by the G-clamp base moiety, rather than by the 2',4'-BNA/LNA sugar moiety. Thus, the high enzymatic stability of ODN- \mathbf{B}^{AEO} may also be useful in cellular applications, such as ON-based therapies.

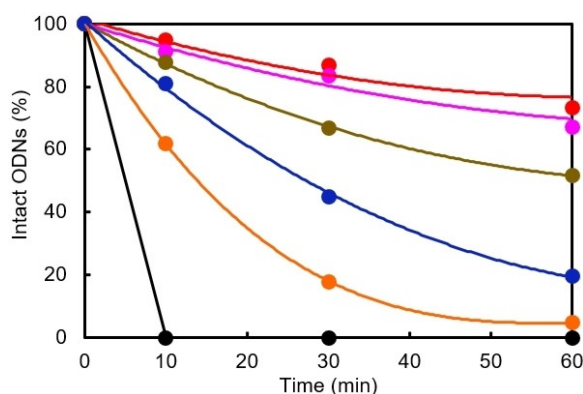


Figure 6. Resistance of ODNs containing \mathbf{B}^{AEO} against 3'-exonuclease. Conditions: 10 mM MgCl_2 , 50 mM Tris-HCl at pH 8.0, $2 \mu\text{M}$ ODN, *C. adamanteus* venom phosphodiesterase ($114 \mu\text{g mL}^{-1}$) at 37°C . ODN sequence: 5'-TTTTTTTTT \mathbf{X} -3'. **X**: **C** (black), **L** (blue), phosphorothiate (PS) R_p isomer (orange), PS S_p isomer (ocher), \mathbf{P}^{AEO} (pink), or \mathbf{B}^{AEO} (red).

Conclusion

We successfully synthesized a \mathbf{B}^{AEO} nucleoside and incorporated it into ODNs. The \mathbf{B}^{AEO} derivative dramatically improved duplex stability in comparison with \mathbf{P}^{AEO} , \mathbf{B}^{H} , \mathbf{P}^{H} , **L**, or **C**. The binding constants (K_b) of ODN- \mathbf{B}^{AEO} for cRNA was 10^4 - and 152-fold higher than those of ODN-**C** and ODN-**L**, respectively. The \mathbf{B}^{AEO} derivative also had base-discrimination abilities that were similar to those of \mathbf{P}^{AEO} . Thermal stabilities of duplexes of \mathbf{P}^{AEO} were the same as or slightly higher than those of duplexes of **L** under molecular crowding PEG(+) conditions, although the thermal stabilities of duplexes of \mathbf{P}^{AEO} were higher than those of duplexes of **L** under PEG(-) conditions. On the other hand, duplexes of \mathbf{B}^{AEO} maintained high thermal stability under both

PEG(+) and PEG(-) conditions compared with that of duplexes of \mathbf{P}^{AEO} . The high enzymatic resistance of \mathbf{B}^{AEO} could offer several advantages in clinical cellular applications. To the best of our knowledge, the \mathbf{B}^{AEO} derivative possesses excellent duplex-forming abilities in all artificial nucleic acids developed to date. Thus, the \mathbf{B}^{AEO} nucleoside is likely to be useful in DNA nanotechnologies and nucleic acid based therapies that require high duplex-forming ability and enzymatic stability.

Experimental Section

General

Dehydrated acetonitrile, CH_2Cl_2 , DMF, pyridine, and THF were purchased from Wako Pure Chemical. Fuji Silysia PSQ-60B, PSQ-100B, or FL-100D were used for column chromatography on silica gel. ^1H , ^{13}C , and ^{31}P NMR spectra were recorded on JEOL JNM-ECS300, JNM-ECS400, and JNM-ECA500 spectrometers. Chemical shift values were reported in ppm relative to internal tetramethylsilane ($\delta = 0.00$ ppm), residual CHD_2OD ($\delta = 3.31$ ppm), CHD_2CN ($\delta = 1.94$ ppm), or $\text{CHD}_2\text{S}(=\text{O})\text{D}_3$ ($\delta = 2.50$ ppm) for ^1H NMR spectroscopy. For ^{13}C NMR spectroscopy, chemical shift values are reported in ppm relative to CDCl_3 ($\delta = 77.2$ ppm), CD_3OD ($\delta = 49.0$ ppm), $[\text{D}_3]\text{acetonitrile}$ ($\delta = 1.32$ ppm), or $[\text{D}_6]\text{DMSO}$ ($\delta = 39.5$ ppm). Chemical shift values were reported in ppm relative to 5% H_3PO_4 ($\delta = 0.00$ ppm) and trifluoroacetic acid ($\delta = -78.5$ ppm) as external standard for ^{31}P and ^{19}F NMR spectroscopy, respectively. IR spectra were recorded on a JASCO FT/IR-4200 spectrometer. Optical rotations were recorded on a JASCO DIP-370 instrument. MALDI-TOF mass spectra were recorded on a JEOL SpiralTOF JMS-S3000 spectrometer.

Synthesis of compound 2

Under an argon atmosphere, Ph_3P (4.30 g, 16.4 mmol) and CCl_4 (80 mL) were added to a solution of **1** (3.40 g, 8.11 mmol) in CH_2Cl_2 (90 mL). The mixture was heated at reflux for 2 h. After the reaction mixture was cooled to room temperature, 2-aminoresorcinol (2.08 g, 16.7 mmol) and DBU (2.4 mL, 16 mmol) were added and stirred at room temperature for 6 h. The reaction mixture was concentrated under reduced pressure, and the residue was dissolved in CHCl_3 . This organic solution was washed with a 5% aqueous solution of citric acid, dried over Na_2SO_4 , and concentrated under reduced pressure. The residue was purified by column chromatography on silica gel ($\text{CHCl}_3/\text{MeOH} = 97/3$ to 95/5) to give **2** as a yellow solid (3.10 g, 73%). $[\alpha]_D^{25} = +14.4$ (c 1.0, CH_3CN); IR (KBr): $\nu_{\text{max}} = 1025, 1057, 1092, 1129, 1232, 1292, 1346, 1372, 1422, 1447, 1500, 1586, 1650, 1758, 1853, 2359, 2569, 2763, 2895, 2955, 3020, 3088, 3299 \text{ cm}^{-1}$; ^1H NMR (400 MHz, CD_3CN): $\delta = 2.06$ (3H, s), 2.14 (3H, s), 3.93, 3.99 (2H, ABq, $J = 8.0$ Hz), 4.37, 4.47 (2H, ABq, $J = 12.0$ Hz), 4.57 (1H, s), 4.94 (1H, s), 5.59 (1H, s), 6.48 (2H, d, $J = 8.0$ Hz), 6.97 (1H, t, $J = 8.0$ Hz), 8.01 (1H, s), 8.05 (1H, s), 9.28 ppm (1H, s); ^{13}C NMR (101 MHz, CD_3CN): $\delta = 20.9, 21.0, 59.7, 71.7, 72.5, 78.5, 86.8, 88.6, 89.2, 109.7, 115.5, 118.3, 128.4, 141.8, 151.1, 153.2, 158.3, 170.7, 171.0$ ppm; HRMS (MALDI): m/z calcd for $\text{C}_{20}\text{H}_{21}\text{N}_3\text{O}_9\text{Br}$ [$M+\text{H}$] $^+$: 526.0456; found: 526.0450.

Synthesis of compound 3

Under an argon atmosphere, Ph_3P (1.72 g, 6.54 mmol) and benzyl-*N*-(2-hydroxyethyl)carbamate (1.28 g, 6.57 mmol), and DEAD (2.95 mL, 16.2 mmol) were added to a solution of **2** (3.10 g, 5.89 mmol) in $\text{CH}_2\text{Cl}_2/\text{THF}$ (130/65 mL). The mixture was heated at

reflux for 5 h. After the addition of a saturated aqueous solution of NaHCO_3 at 0°C , the mixture was extracted with CHCl_3 . The organic layer was washed with a saturated aqueous solution of NaHCO_3 and H_2O , dried over Na_2SO_4 , and then concentrated under reduced pressure. The residue was purified by column chromatography on silica gel (1: $\text{CHCl}_3/\text{AcOEt}=8/2$ to $6/4$; 2: $\text{CHCl}_3/\text{MeOH}=95/5$ to $93/7$) to give **3** as a yellow foam (3.94 g, 95%). $[\alpha]_{\text{D}}^{26} = +5.5$ (c 1.0, CHCl_3); IR (KBr): $\nu_{\text{max}}=1058, 1094, 1129, 1238, 1281, 1331, 1369, 1391, 1419, 1508, 1570, 1622, 1677, 1716, 1749, 2359, 2570, 2765, 2890, 2954, 3011, 3086, 3329\text{ cm}^{-1}$; $^1\text{H NMR}$ (400 MHz, CDCl_3): $\delta=2.12$ (s, 3H), 2.20 (s, 3H), 3.66–3.70 (m, 2H), 3.96, 4.01 (ABq, $J=8.0$ Hz, 2H), 4.10–4.16 (m, 2H), 4.39, 4.46 (ABq, $J=12.0$ Hz, 2H), 4.73 (s, 1H), 4.85 (s, 1H), 5.12 (s, 2H), 5.48–5.51 (m, 1H), 5.70 (s, 1H), 6.40 (d, $J=8.0$ Hz, 1H), 6.67 (dd, $J=0.9, 8.4$ Hz, 1H), 7.00 (t, $J=8.0$ Hz, 1H), 7.30–7.35 (m, 5H), 7.92 (s, 1H), 8.09 (s, 1H), 11.05 ppm (s, 1H); $^{13}\text{C NMR}$ (100.5 MHz, CDCl_3): $\delta=20.9, 20.9, 40.8, 58.5, 67.0, 67.7, 70.6, 71.7, 77.4, 77.6, 85.8, 85.8, 87.8, 89.0, 102.6, 114.2, 115.6, 127.3, 128.3, 128.3, 128.6, 136.4, 140.1, 150.1, 150.2, 151.8, 156.3, 156.5, 169.7, 170.1$ ppm; HRMS (MALDI): m/z calcd for $\text{C}_{30}\text{H}_{31}\text{N}_4\text{O}_{11}\text{NaBr}$ [$M+\text{Na}$] $^+$: 725.1065; found: 725.1085.

Synthesis of compound 5

A 7 M solution of NH_3/MeOH was added to **3** (3.50 g, 4.98 mmol). The mixture reacted at room temperature for 3 h under an argon atmosphere and was concentrated under reduced pressure. Residue **4** (3.00 g) was used without purification in the next reaction. Under an argon atmosphere, DBU (800 μL , 5.35 mmol) was added to a solution of **4** (3.00 g) in EtOH (300 mL), and the mixture was heated at reflux for 5 h. The reaction mixture was concentrated under reduced pressure, and the residue was dissolved in CH_2Cl_2 . The organic solution was washed with a saturated aqueous solution of NaHCO_3 , dried over with Na_2SO_4 , and concentrated under reduced pressure. The residue was purified by column chromatography on silica gel ($\text{CHCl}_3/\text{MeOH}=97/3$ to $90/10$) to give **5** as an orange foam (1.53 g, 57% in 2 steps). $[\alpha]_{\text{D}}^{26} = -7.3$ (c 1.0, CHCl_3); IR (KBr): $\nu_{\text{max}}=1015, 1055, 1075, 1098, 1147, 1233, 1254, 1280, 1333, 1363, 1382, 1418, 1476, 1510, 1559, 1611, 1671, 1699, 2359, 2884, 2947, 3091, 3275\text{ cm}^{-1}$; $^1\text{H NMR}$ (400 MHz, CD_3OD): $\delta=3.48$ – 3.59 (m, 2H), 3.75, 3.95 (ABq, $J=6.0$ Hz, 2H), 3.90 (s, 2H), 4.02 (t, $J=4.0$ Hz, 2H), 4.08 (s, 1H), 4.31 (s, 1H), 5.10, 5.14 (ABq, $J=12.0$ Hz, 2H), 5.49 (s, 1H), 6.38 (d, $J=8.0$ Hz, 1H), 6.54 (d, $J=8.0$ Hz, 1H), 6.79 (t, $J=10.0$ Hz, 1H), 7.23–7.33 (m, 5H), 7.51 ppm (s, 1H); $^{13}\text{C NMR}$ (100.5 MHz, CD_3OD): $\delta=41.2, 57.6, 67.5, 69.6, 70.2, 72.4, 80.7, 88.7, 90.4, 108.2, 109.3, 116.8, 123.1, 124.9, 128.6, 128.9, 129.4, 129.6, 138.4, 144.3, 147.8, 155.8, 156.2, 159.1$ ppm; HRMS (MALDI): m/z calcd for $\text{C}_{26}\text{H}_{26}\text{N}_4\text{O}_9\text{Na}$ [$M+\text{Na}$] $^+$: 561.1592; found: 561.1595.

Synthesis of compound 6

$\text{Pd}(\text{OH})_2/\text{C}$ (20 mg) and cyclohexene (8 mL) were added to a solution of **5** (45 mg, 0.084 mmol) in MeOH (10 mL), and the mixture was heated at reflux for 3 h. After the reaction mixture was cooled to room temperature, the mixture was filtered to remove $\text{Pd}(\text{OH})_2/\text{C}$. The residue was concentrated under reduced pressure to give **6** as a yellow solid (32 mg, 93%). $[\alpha]_{\text{D}}^{27} = -3.7$ (c 1.0, DMSO); IR (KBr): $\nu_{\text{max}}=1009, 1052, 1075, 1094, 1120, 1130, 1202, 1237, 1261, 1282, 1316, 1335, 1368, 1411, 1435, 1475, 1512, 1562, 1608, 1634, 1666, 2343, 2954, 3302\text{ cm}^{-1}$; $^1\text{H NMR}$ (500 MHz, $[\text{D}_6]\text{DMSO}$): $\delta=2.85$ – 2.88 (m, 2H), 3.61, 3.80 (ABq, $J=6.0$ Hz, 2H), 3.73 (s, 2H), 3.87–3.89 (m, 2/10H), 3.91 (s, 8/10H), 3.92 (s, 2/10H), 4.03–4.06 (m, 8/10H), 4.11 (s, 8/10H), 4.12 (s, 2/10H), 5.32 (s, 8/10H), 5.35 (s, 2/10H), 6.38 (d, $J=4.0$ Hz, 8/10H), 6.45 (d, $J=8.0$ Hz, 2/10H), 6.56 (d, $J=8.0$ Hz, 8/10H), 6.61 (d, $J=8.0$ Hz, 2/10H), 6.70 (t, $J=8.0$ Hz, 8/10H), 6.80 (t,

$J=6.0$ Hz, 2/10H), 7.36 (s, 8/10H), 7.47 ppm (s, 2/10H); $^{13}\text{C NMR}$ (100.5 MHz, $[\text{D}_6]\text{DMSO}$): $\delta=51.1, 55.7, 68.3, 70.9, 73.6, 78.8, 86.6, 88.8, 108.1, 109.3, 117.3, 123.1, 123.2, 126.7, 142.6, 146.9, 152.5, 153.4$ ppm; HRMS (MALDI): m/z calcd for $\text{C}_{18}\text{H}_{20}\text{N}_4\text{O}_7\text{Na}$ [$M+\text{Na}$] $^+$: 427.1224; found: 427.1226.

Synthesis of compound 8

Under an argon atmosphere, TFAA (12 mL, 3.8 mmol) was added to a solution of **6** (641 mg, 1.56 mmol) in anhydrous pyridine (60 mL) at 0°C . The mixture was stirred at room temperature for 2 h. The reaction mixture was concentrated to give crude **7** (702 mg), which was used in the next step without purification. Under an argon atmosphere, DMTrCl (1.25 g, 3.64 mmol) in CH_2Cl_2 (5 mL) was added to a solution of AgOTf (936 mg, 3.64 mmol) in CH_2Cl_2 (25 mL), and the mixture was stirred at room temperature for 1 h to give DMTrOTf solution. Then, DMTrOTf solution (17 mL) was added to a solution of **7** in anhydrous 2,6-lutidine (35 mL) at 0°C , and the mixture was stirred for 2 h. After the addition of H_2O at 0°C , the mixture was extracted with AcOEt. The organic layer was washed with a saturated aqueous solution of NaHCO_3 and an aqueous solution of copper(II) sulfate (3.0 g in 20 mL H_2O) to remove 2,6-lutidine, dried over Na_2SO_4 , and then concentrated under reduced pressure. The residue was purified by column chromatography on silica gel (0.5% triethylamine in *n*-hexane/AcOEt = 2/8 to 0/1) to give **8** as a yellow foam (597 mg, 47% in 2 steps). $[\alpha]_{\text{D}}^{25} = -8.1$ (c 1.0, CH_3CN); IR (KBr): $\nu_{\text{max}}=1017, 1057, 1081, 1104, 1155, 1190, 1228, 1261, 1287, 1329, 1363, 1383, 1418, 1446, 1480, 1517, 1566, 1612, 1676, 1726, 1969, 2048, 2177, 2300, 2359, 2428, 2548, 2601, 2837, 2949, 3091, 3275\text{ cm}^{-1}$; $^1\text{H NMR}$ (400 MHz, CD_3CN): $\delta=3.39$ (s, 2H), 3.66, 3.77 (ABq, $J=8.0$ Hz, 2H), 3.68–3.72 (m, 2H), 3.74 (s, 6H), 4.03–4.11 (m, 2H), 4.18 (d, $J=4.0$ Hz, 1H), 4.30 (d, $J=4.0$ Hz, 1H), 4.39 (s, 1H), 5.40 (s, 1H), 6.21 (dd, $J=8.3, 0.8$ Hz, 1H), 6.49 (dd, $J=8.4, 0.7$ Hz, 1H), 6.75 (t, $J=8.0$ Hz, 1H), 6.88 (m, 4H), 7.23–7.27 (m, 1H), 7.31–7.38 (m, 6H), 7.47–7.50 (m, 3H), 8.00 (s, 1H), 8.24 ppm (t, $J=6.0$ Hz, 1H); $^{13}\text{C NMR}$ (100.5 MHz, CD_3CN): $\delta=39.9, 55.9, 59.1, 68.1, 70.4, 72.4, 80.0, 87.2, 87.2, 88.4, 88.6, 88.6, 107.6, 109.1, 114.1, 115.7, 116.4, 123.1, 124.4, 127.9, 128.7, 129.0, 131.0, 136.6, 136.6, 136.6, 143.6, 143.6, 145.8, 146.9, 154.8, 155.0, 158.0, 158.4, 159.7$ ppm; $^{19}\text{F NMR}$ (376.2 MHz, CD_3CN): $\delta=-77.2$; HRMS (MALDI): m/z calcd for $\text{C}_{41}\text{H}_{37}\text{N}_4\text{O}_{10}\text{F}_3\text{Na}$ [$M+\text{Na}$] $^+$: 825.2354; found: 825.2364.

Synthesis of compound 9

Under an argon atmosphere, DIPEA (42 μL , 0.24 mmol) and *N,N*-diisopropylamino-2-cyanoethylphosphino chloridite (32 μL , 0.14 mmol) were added to a solution of **8** (97 mg, 0.12 mmol) in CH_2Cl_2 (2 mL) at 0°C , and the mixture was stirred for 2 h at room temperature. After the addition of H_2O at 0°C , the mixture was extracted with AcOEt. The organic extracts were washed with a saturated aqueous solution of NaHCO_3 , water, and brine; dried over Na_2SO_4 ; and then concentrated under reduced pressure. The residue was purified by column chromatography on silica gel (0.5% triethylamine in *n*-hexane/AcOEt = 3/7 to 2/8) to give **9** as a yellow foam (93 mg, 77%). $^1\text{H NMR}$ (400 MHz, CDCl_3): $\delta=0.97$ – 1.29 (m, 12H), 2.38 (t, $J=6.0$ Hz, 7/8H), 2.55 (t, $J=6.0$ Hz, 1/8H), 3.36 (d, $J=12.0$ Hz, 8/10H), 3.40 (d, $J=12.0$ Hz, 2/10H), 3.46–3.57 (m, 5H), 3.76–3.82 (m, 10H), 4.13–4.17 (m, 2H), 4.25 (d, $J=8.0$ Hz, 2/10H), 4.33 (d, $J=8.0$ Hz, 8/10H), 4.60 (s, 17/20H), 4.64 (s, 3/20H), 5.59 (s, 3/20H), 5.61 (s, 17/20H), 6.28 (d, $J=8.0$ Hz, 1H), 6.45 (d, $J=8.0$ Hz, 1H), 6.79 (t, $J=12.0$ Hz, 1H), 6.83–6.87 (m, 4H), 7.22 (t, $J=8.0$ Hz, 1H), 7.31 (t, $J=8.0$ Hz, 2H), 7.36 (d, $J=8.0$ Hz, 4H), 7.47 (d, $J=8.0$ Hz, 2H), 7.54 (s, 1H), 8.29 (s, 1H), 8.40 ppm (s, 1H); $^{19}\text{F NMR}$

(376.2 MHz, CDCl₃): $\delta = -76.8, -76.7$ ppm; ³¹P NMR (161.8 MHz, CDCl₃): $\delta = 149.1, 149.4$ ppm; HRMS (MALDI): *m/z* calcd for C₅₀H₅₄N₆O₁₁F₃NaP [M + Na]⁺: 1025.3433; found: 1025.3440.

Synthesis of ODNs containing B^{AEO}

Syntheses of the ODNs containing B^{AEO} was performed on an automated DNA synthesizer (Gene Design, nS-8) at the 0.2 μ mol scale. Activator 42[®] was used as the activator. The coupling time of the standard phosphoramidite coupling protocol was increased from 30 s to 12 min. The B^{AEO} phosphoramidite **9** was prepared with 0.10 M acetonitrile/THF (v/v, 3:1). The ON synthesis was performed in the DMTr-on mode. CPG-supported ODNs were cleaved and the protecting groups of the nucleobases were removed with 50 mM K₂CO₃ in MeOH at RT for 4 h. The DMTr group in ODNs were detritylated and purified with a Sep-Pak[®] Plus C18 Cartridge and Sep-Pak[®] Plus C18 Environmental Cartridge (Waters) [washed with 10% acetonitrile aqueous solution, detritylated with 0.5% aqueous trifluoroacetic acid solution, and eluted with 35% aqueous MeOH solution]. ODNs were purified by means of reverse-phase HPLC on a Waters XBridge[™] OST C18 2.5 μ m (10 \times 50 mm) with 0.1 M triethylammonium acetate buffer (pH 7.0) (buffer a) and acetonitrile (buffer b). The purified ODNs were analyzed by means of reverse-phase HPLC on a Waters XBridge[™] OST C18 2.5 μ m (4.6 \times 50 mm) column. The structures of ODNs were determined by means of MALDI-TOF MS (Bruker Daltonics AutoflexII TOF/TOF mass spectrometer).

Thermal denaturation experiments

UV melting experiments were carried out on Shimadzu UV-1650PC and UV-1800 spectrometers equipped with *T_m* analysis accessory quartz cuvettes of 1 cm in optical path length. The UV melting profiles were recorded in 2 mM sodium phosphate buffer (pH 7.2) containing 20 mM NaCl to give a final concentration of each ON of 2 μ M. The samples were annealed by heating at 100 °C followed by slow cooling to room temperature. The melting profile was recorded at 260 nm from 5 to 90 °C at a scan rate of 0.5 °C min⁻¹. The *T_m* values were calculated as the temperature for the half of the formed duplex to dissociate based on the first derivative of the melting curve.

CD measurements

CD spectra were measured by using a JASCO J-720W spectrophotometer. These spectra were recorded at 10 °C in a quartz cuvette with a 1 cm optical path length. The samples were prepared in the same manner as those described in the UV melting experiments. The molar ellipticity was calculated from the equation $[\theta] = \theta/cl$, in which θ is the relative intensity, *c* is the sample concentration, and *l* is the cell path length in cm.

Molecular modeling

MD calculations of duplexes containing B^{AEO} were conducted by using MacroModel software (Schrödinger, LLC), with the OPLS3 force field (in water at 300 K for 20 ns).

Fluorescence measurements

Fluorescence spectra were obtained on a HITACHI F-7000 fluorescence spectrophotometer. The spectra were recorded at 25 °C with a quartz cuvette of 1 cm in optical path length.

Thermodynamic analysis

The UV melting profiles for thermodynamic analysis were recorded in 2 mM sodium phosphate buffer (pH 7.2) containing 20 mM NaCl to achieve a final concentration of each ON in 0.45, 0.74, 1.22, and 2.00 μ M for 130 μ L, and 3.26 and 6.80 μ M for 50 μ L. These samples were annealed by heating at 100 °C followed by slow cooling to room temperature. The melting profile was recorded by using the same method as that described for thermal denaturing experiments. The van't Hoff plots were recorded as *T_m* values at each concentration, and each value of ΔH , ΔS , and ΔG was calculated according to Equations (1) and (2):

$$1/T_m = (R/\Delta H)\ln(C_t/4) + \Delta S/\Delta H \quad (1)$$

$$\Delta G = \Delta H - T\Delta S \quad (2)$$

in which *R* indicates the gas constant and *C_t* indicates the total concentration of ONs.

Enzymatic resistance of ODNs

Solutions (300 μ L, 2 μ M) of ODNs-X containing 10 mM MgCl₂ and 50 mM Trip-HCl buffer (pH 8.0) were reacted with 3'-exonuclease (0.13 μ g mL⁻¹) at 37 °C. Aliquots (50 μ L) of each sample were removed at 10, 30, and 60 min and heated at 90 °C for 5 min to inactivate 3'-exonuclease. The amounts of intact ODNs were quantified by means of reverse-phase HPLC.

Acknowledgements

This work was supported by the Core Research for Evolutional Science and Technology (CREST) program of the Japan Science and Technology Agency (JST), JSPS KAKENHI (grant numbers 15K08024 and 20K05706 (awarded to O.N.)), and the Basic Science and Platform Technology Program for Innovative Biological Medicine from the Japan Agency for Medical Research and Development (AMED) under grant number JP18am0301004. This research was also partially supported by the Platform Project for Supporting Drug Discovery and Life Science Research from AMED.

Conflict of interest

The authors declare no conflict of interest.

Keywords: bridged nucleic acids • enzyme resistance • nucleobases • pi interactions • synthesis design

- [1] N. C. Seeman, H. F. Sleiman, *Nat. Rev. Mater.* **2017**, *3*, 17068.
- [2] K. Morihiro, Y. Kasahara, S. Obika, *Mol. BioSyst.* **2017**, *13*, 235–245.
- [3] a) S. Obika, *Chem. Pharm. Bull.* **2004**, *52*, 1399–1140; b) F. Debart, C. Dupouy, J.-J. Vasseur, *Beilstein J. Org. Chem.* **2018**, *14*, 436–469.
- [4] a) K.-Y. Lin, R. J. Jones, M. Matteucci, *J. Am. Chem. Soc.* **1995**, *117*, 3873–3874; b) W. M. Flanagan, R. W. Wagner, D. Grant, K. Y. Lin, M. D. Matteucci, *Nat. Biotechnol.* **1999**, *17*, 48–52.
- [5] a) K.-Y. Lin, M. D. Matteucci, *J. Am. Chem. Soc.* **1998**, *120*, 8531–8532; b) W. M. Flanagan, J. J. Wolf, P. Olson, D. Grant, K.-Y. Lin, R. W. Wagner, M. D. Matteucci, *Proc. Natl. Acad. Sci. USA* **1999**, *96*, 3513–3518; c) S. C. Holmes, A. A. Arzumanov, M. J. Gait, *Nucleic Acids Res.* **2003**, *31*, 2759–2768; d) J.-A. Ortega, J. R. N. Blas, M. Orozco, A. Grandas, E. Pedrosa, J. Robles, *Org. Lett.* **2007**, *9*, 4503–4506; e) R. Stanton, S. Sciabola, C. Sal-

- atto, Y. Weng, D. Moshinsky, J. Little, E. Walters, J. Kreeger, D. DiMattia, T. Chen, T. Clark, M. Liu, J. Qian, M. Roy, R. Dullea, *Nucleic Acid Ther.* **2012**, *22*, 344–359.
- [6] a) B. J. Rodgers, N. A. Elsharif, N. Vashisht, M. M. Mingus, M. A. Mulvahill, G. Stengel, R. D. Kuchta, B. W. Purse, *Chem. Eur. J.* **2014**, *20*, 2010–2015; b) C. P. Lawson, A. F. Füchtbauer, M. S. Wranner, T. Giraud, T. Floyd, B. Dumat, N. K. Andersen, A. H. El-Sagheer, T. Brown, H. Gradén, L. M. Wilhelmsson, M. Grötl, *Sci. Rep.* **2018**, *8*, 13970; c) M. Bood, S. Sarangamath, M. S. Wranner, M. Grötl, L. M. Wilhelmsson, *Beilstein J. Org. Chem.* **2018**, *14*, 114–129.
- [7] A. Fujii, O. Nakagawa, Y. Kishimoto, Y. Nakatsuji, N. Nozaki, S. Obika, *ChemBioChem* **2020**, *21*, 860–864.
- [8] A. Fujii, O. Nakagawa, Y. Kishimoto, T. Okuda, Y. Nakatsuji, N. Nozaki, Y. Kasahara, S. Obika, *Chem. Eur. J.* **2019**, *25*, 7443–7448.
- [9] Y. Kishimoto, A. Fujii, O. Nakagawa, T. Nagata, T. Yokota, Y. Hari, S. Obika, *Org. Biomol. Chem.* **2017**, *15*, 8145–8152.
- [10] a) S. Obika, D. Nanbu, Y. Hari, K. Morio, Y. In, T. Ishida, T. Imanishi, *Tetrahedron Lett.* **1997**, *38*, 8735–8738; b) S. Obika, D. Nanbu, Y. Hari, J. Andoh, K. Morio, T. Doi, T. Imanishi, *Tetrahedron Lett.* **1998**, *39*, 5401–5404.
- [11] a) S. K. Singh, P. Nielsen, A. A. Koshkin, J. Wengel, *Chem. Commun.* **1998**, 455–456; b) A. A. Koshkin, S. K. Singh, P. Nielsen, V. K. Rajwanshi, R. Kumar, M. Meldgaard, C. E. Olsen, J. Wengel, *Tetrahedron* **1998**, *54*, 3607–3630.
- [12] a) P. M. McTigue, R. J. Peterson, J. D. Kahn, *Biochemistry* **2004**, *43*, 5388–5405; b) H. Kaur, A. Arora, J. Wengel, S. Maiti, *Biochemistry* **2006**, *45*, 7347–7355; c) U. Christensen, *Biosci. Rep.* **2007**, *27*, 327–333; d) H. Kaur, J. Wengel, S. Maiti, *Biochemistry* **2008**, *47*, 1218–1227; e) E. Kierzek, A. Pasternak, K. Pasternak, Z. Gdaniec, I. Yildirim, D. H. Turner, R. Kierzek, *Biochemistry* **2009**, *48*, 4377–4387.
- [13] a) S. Nakano, H. Karimata, T. Ohmichi, J. Kawakami, N. Sugimoto, *J. Am. Chem. Soc.* **2004**, *126*, 14330–14331; b) D. Miyoshi, N. Sugimoto, *Biochimie* **2008**, *90*, 1040–1051; c) S. Nakano, D. Miyoshi, N. Sugimoto, *Chem. Rev.* **2014**, *114*, 2733–2758; d) S. Nakano, N. Sugimoto, *Mol. Bio-Syst.* **2017**, *13*, 32–41; e) S. Ghosh, S. Takahashi, T. Endoh, H. Tateishi-Karimata, S. Hazra, N. Sugimoto, *Nucleic Acids Res.* **2019**, *47*, 3284–3294.
- [14] a) L. M. Wilhelmsson, A. Holmén, P. Lincoln, P. E. Nielsen, B. Nordén, *J. Am. Chem. Soc.* **2001**, *123*, 2434–2435; b) L. M. Wilhelmsson, P. Sandin, A. Holmén, B. Albinsson, P. Lincoln, B. Nordén, *J. Phys. Chem. B* **2003**, *107*, 9094–9101; c) K. C. Engman, P. Sandin, S. Osborne, T. Brown, M. Billeter, P. Lincoln, B. Nordén, B. Albinsson, L. M. Wilhelmsson, *Nucleic Acids Res.* **2004**, *32*, 5087–5095; d) P. Sandin, L. M. Wilhelmsson, P. Lincoln, V. E. C. Powers, T. Brown, B. Albinsson, *Nucleic Acids Res.* **2005**, *33*, 5019–5025; e) P. Sandin, P. Lincoln, T. Brown, L. M. Wilhelmsson, *Nat. Protoc.* **2007**, *2*, 615–623; f) P. Sandin, K. Börjesson, H. Li, J. Mårtensson, T. Brown, L. M. Wilhelmsson, B. Albinsson, *Nucleic Acids Res.* **2008**, *36*, 157–167; g) K. Börjesson, S. Preus, A. H. El-Sagheer, T. Brown, B. Albinsson, L. M. Wilhelmsson, *J. Am. Chem. Soc.* **2009**, *131*, 4288–4293; h) H. Gardarsson, A. S. Kale, S. T. Sigurdsson, *ChemBioChem* **2011**, *12*, 567–575; i) B. Dumat, A. F. Larsen, L. M. Wilhelmsson, *Nucleic Acids Res.* **2016**, *44*, e101; j) A. F. Füchtbauer, S. Preus, K. Börjesson, S. A. McPhee, D. M. J. Lilley, L. M. Wilhelmsson, *Sci. Rep.* **2017**, *7*, 2393.
- [15] M. A. Maier, J. M. Leeds, G. Balow, R. H. Springer, R. Bharadwaj, M. Manoharan, *Biochemistry* **2002**, *41*, 1323–1327.
- [16] a) O. Nakagawa, S. Ono, Z. Li, A. Tsujimoto, S. Sasaki, *Angew. Chem. Int. Ed.* **2007**, *46*, 4500–4503; *Angew. Chem.* **2007**, *119*, 4584–4587; b) Y. Koga, Y. Fuchi, O. Nakagawa, S. Sasaki, *Tetrahedron* **2011**, *67*, 6746–6752.
- [17] C. A. M. Seidel, A. Schulz, M. H. M. Sauer, *J. Phys. Chem.* **1996**, *100*, 5541–5553.

Manuscript received: August 31, 2020

Accepted manuscript online: October 14, 2020

Version of record online: December 21, 2020